A 160-GHz Radar With Flexible Antenna Used as a Sniffer Probe

Martin Geiger, *Student Member, IEEE*, Martin Hitzler, *Student Member, IEEE*, Stefan Saulig, *Student Member, IEEE*, Johannes Iberle, Philipp Hügler, *Student Member, IEEE*, and Christian Waldschmidt, *Senior Member, IEEE*

***Abstract*— In radar measurements, the observed area is limited by the antenna beamwidth, and due to the usually fixed transceiver position, only unhidden targets in a small observation area can be detected. Furthermore, bulky lens dimensions prevent the use of radar systems in constricted surroundings despite the small dimensions of microwave monolithic integrated circuit (MMIC) radars. To avoid this issue, a new system concept for a flexible and low-cost 160-GHz radar sniffer probe is presented. The flexible sniffer probe is an extremely low-loss dielectric waveguide with a dielectric elliptical lens (28 dBi) at the end. The dielectric waveguide has dielectric losses of 4.5 dB/m at 160 GHz and high flexibility, supporting bending radii of 1.5 cm with negligible losses. To feed the dielectric waveguide, a metallic waveguide with a duplexer is used, which is fed by a special MMIC-to-metallic waveguide transition. The proposed system expands the known radar measurement scenarios with new industrial, medical, and security applications.**

***Index Terms*— Flexible radar sensor, radar sniffer probe, dielectric waveguide, lens antenna, MMIC, rectangular waveguide coupler, millimeter wave.**

I. Introduction

RADAR systems are known for their robustness in distances and velocity measurements. Therefore, the demand for cheap and compact radar systems for industrial applications like level measurements in tanks [1], surveillance of conveyor belts, or sensors in the automotive industry [2], [3] increases. By integrating complete radar systems on chip in silicon-germanium (SiGe), a cost efficient production is possible for different frequencies from 60 GHz [4] over 90 GHz [5] up to more than 100 GHz [6], [7]. With on-chip antennas and antennas-in-package, the compactness of radar systems is further increased and lossy MMIC-to-PCB transitions are avoided [8]–[10].

For a large dynamic range in radar measurements a high gain antenna is needed besides a good MMIC performance. Thus, additional lenses are used located above the MMIC with on-chip antennas to achieve a high gain and a high SNR [11], [12]. Despite the compactness of the MMIC, the size of the overall system is increased considerably when using bulky lenses. The on-chip antenna gain can also be improved by more compact MMIC extensions like a horn [13] or a bulk lens [7]. However, these radars are not flexible to go around obstacles and detect hidden targets and can therefore only detect targets within the beamwidth of the antenna.

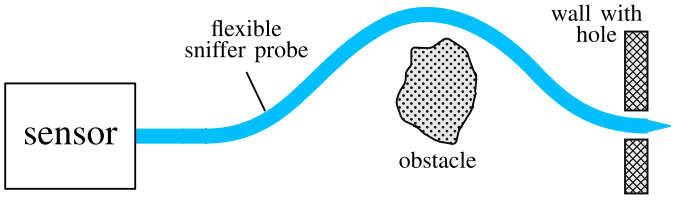

Fig. 1. Schematic view of a flexible sniffer probe measuring around an obstacle.

Flexible sensor heads are known from optics [14] or at low frequencies, which are commonly measured with flexible oscilloscope probes. They offer the possibility to move the sensor arbitrarily and measure directly at the desired position. As shown in Fig. 1 such sniffer probes are suited to go around obstacles or to move through small holes in pipes and walls. Additionally, the measurement probe can be spatially separated from the electronics on the printed circuit board (PCB), which is of interest in dirty, humid, or flammable surroundings. For radar applications a flexible sniffer probe entails benefits and enables to measure in areas, which are difficult to access for common radar sensors.

A simple solution for a radar sniffer probe would be a system with flexible IF and DC cables connected to a compact PCB with MMIC and on-chip antenna. Though, this system concept has still bulky dimensions and parts of the electronics are not spatially separated from the measurement scenario.

A second approach would be a flexible antenna as radar sniffer probe. Compared to the before mentioned system, only the antenna with smaller dimensions is moved in measurements. Thereby, the system offers a larger variety of application scenarios. However, the radar sniffer probe requires a suitable waveguide. Microstrip lines are usually on rigid substrates and have high losses at frequencies above 100 GHz. Metallic rectangular waveguides are commonly used in the mm-wave range, but also lack the required flexibility. Instead, flexible dielectric waveguides are used for frequencies above 100 GHz in measurement setups [15] and communication links [16], [17]. These waveguides have extremely low losses, are simple to produce, and are suited for a sniffer probe.

Manuscript received May 2, 2017; revised June 2, 2017; accepted June 12, 2017. Date of publication June 21, 2017; date of current version July 21, 2017. This work was supported by the Ministry for Science, Research and Arts Baden-Württemberg through the project ZAFH MikroSens. The associate editor coordinating the review of this paper and approving it for publication was Dr. Lorenzo Lo Monte. *(Corresponding author: Martin Geiger.)*

The authors are with the Institute of Microwave Engineering, Ulm University, 89081 Ulm, Germany (e-mail: martin-2.geiger@uni-ulm.de).

Digital Object Identifier 10.1109/JSEN.2017.2718100

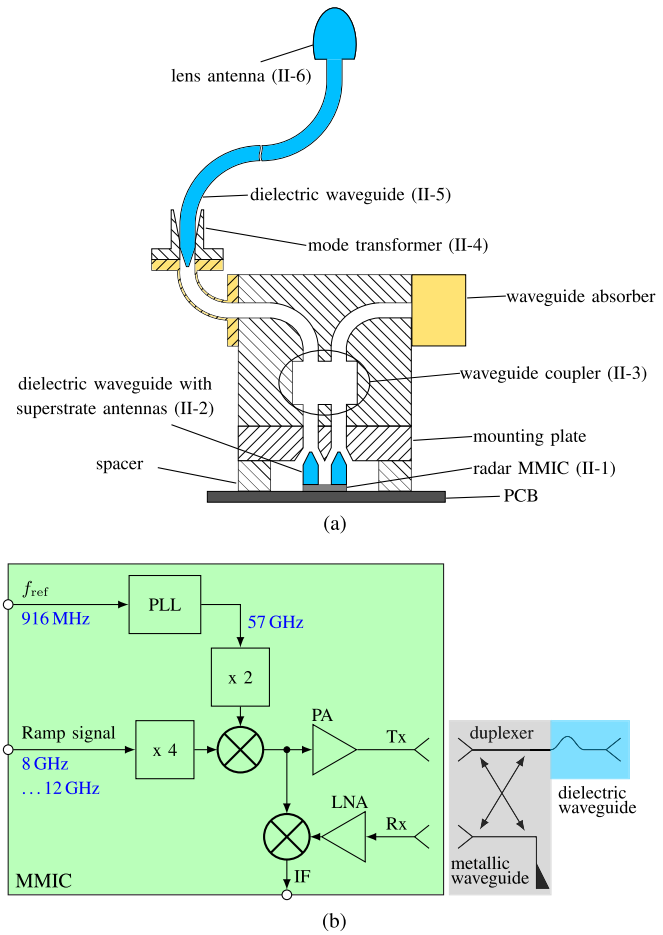

Fig. 2. a) System concept and b) block diagram of the bistatic radar MMIC with transition to the monostatic dielectric waveguide. For MMIC details see [18].

In this paper a new system concept for a 160-GHz radar MMIC with a flexible sniffer probe and the interconnection of the components is presented. At first, the overall system concept with its components, the MMIC, transition from MMIC to metallic waveguide, duplexer, transition from metallic to dielectric waveguide, the lens antenna, and the dielectric waveguide are explained and characterized. The robustness of the system towards influences on the flexible waveguide and the SNR are shown in Section III. Afterwards, two new possible radar applications are described and shown including real measurement scenarios in Section IV.

II. System Concept

The proposed system concept setup is shown in Fig. 2. A dielectric lens antenna on a flexible dielectric waveguide is used as a sniffer probe to detect targets. Several components are needed for the transmission of the signal from the radar MMIC to the antenna.

The signal from the radar MMIC [18] couples through a superstrate antenna into a tapered dielectric waveguide. The dielectric waveguide radiates the signal in a widened metallic waveguide [19]. Since the radar MMIC is bistatic, a waveguide coupler acts as a duplexer. This component is unnecessary for monostatic MMICs. A mode transformer is used for the transition from the metallic waveguide to the dielectric waveguide. A dielectric lens antenna, made of the same material as the dielectric waveguide, is plugged on the flexible dielectric waveguide. The following list explains the required components in detail.

TABLE I
Important System Parameters

MMIC	
Technology	SiGe
Frequency	156 GHz
Bandwidth	16 GHz
Phase noise at 1 MHz offset	−89 dBc/Hz
Transmit power at antenna input	5 dBm
Chip area	2 mm^2
Metallic waveguide	
IL transition MMIC-to-waveguide	3 dB
IL duplexer	3 dB
IL mode transformer	0.4 dB
Dielectric Waveguide	
Attenuation dielectric waveguide	4.5 dB/m
Gain dielectric lens antenna	28 dBi

1) 160 GHz Radar MMIC [18]: The radar MMIC is an ultracompact bistatic FMCW radar chip with low phase noise due to its frequency offset synthesizer. The advantageous chip architecture enables ramp bandwidths up to 16 GHz which makes a high range resolution possible. With the integrated antennas on chip, lossy mm-wave interconnects to PCB are avoided. The most important MMIC parameters are listed in Table I.

2) Transition MMIC to Metallic Waveguide [19]: In order to support a monostatic sniffer probe with a bistatic chip architecture a duplexer as well as a suitable transition from the on-chip antenna to the dielectric sniffer probe are required. As metallic waveguide couplers and metallic waveguide-to-dielectric waveguide transitions are well known, metallic waveguide technology is suitable solution for these components. Therefore, a transition from MMIC to metallic waveguide is required.

In this case, an on-chip antenna and a $\lambda/2$ patch resonator on a quartz glass carrier couples the wave with an efficiency of about 50% in a dielectric waveguide made of PMMA. The second part, the transition from the dielectric waveguide to the metallic waveguide, is non-resonant and broadband. The tapered end of the dielectric waveguide radiates into a widened metallic waveguide and has an insertion loss (IL) of 3 dB. Consequently, the chip and the metallic waveguide are mechanically decoupled, and thermal or mechanical stress in the waveguide components do not affect the MMIC. With this transition the other components can be bolted together on a stable platform. For this reason, a direct mechanical connection between sniffer probe and chip with lower transmission losses was avoided in the system concept.

3) Duplexer [20]: To change the system architecture to a monostatic radar, a duplexer in rectangular waveguide technology is used. The wideband hybrid-coupler is fabricated in split-block design with an isolation of more than 20 dB.

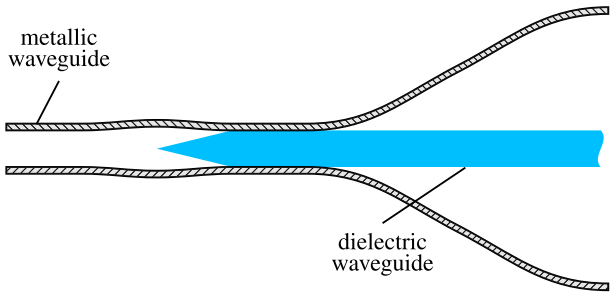

Fig. 3. Schematic view of the mode transformer for the transition from metallic waveguide to dielectric waveguide.

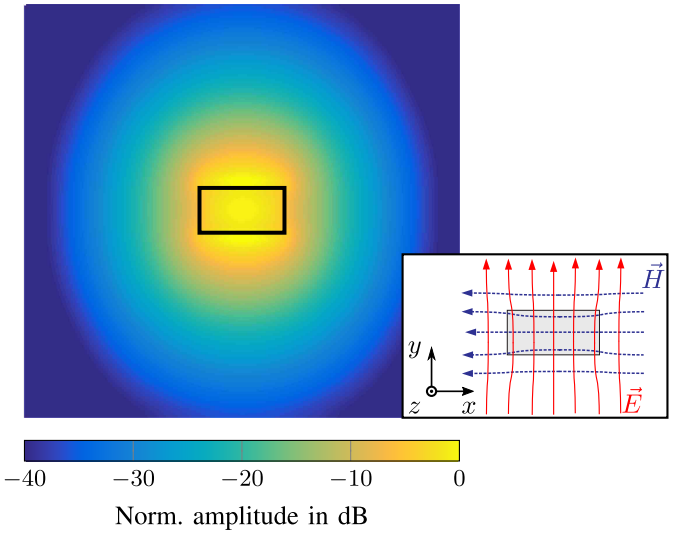

Fig. 4. E-field distribution of the fundamental HE_{11} mode in a dielectric waveguide with polarization in y-direction.

Between 140 GHz and 175 GHz the inserted wave is equally split to the coupled ports. A waveguide absorber is used to avoid reflections at the unused port 4.

4) Mode Transformer: For the transition from the metallic waveguide to the dielectric waveguide a mode transformer is used as shown in Fig. 3. Since the field distribution of the fundamental HE_{11} mode in the dielectric waveguide and the TE_{10} mode in the metallic waveguide are very similar, a tapered horn as proposed in [21] was realized. A dielectric waveguide is placed in the metallic waveguide just before the horn. A tapered dielectric waveguide improves the impedance matching. The measured insertion loss of 0.4 dB was achieved with a smooth gradient of the horn.

5) Dielectric Waveguide: The novel aspect of this radar sensor concept is the flexible sniffer probe. The flexibility is defined by the dielectric waveguide. Therefore, its mechanical and electrical characteristics should be examined in more detail.

The dielectric waveguide is mainly used in the mm-wave range [15]–[17], [22] as well as in optical applications [23]. In Fig. 4 the fundamental mode of the dielectric waveguide, the HE_{11} mode, is shown (also referred to as E_{11}^{y} mode [24]). In contrast to the metallic waveguide the field components are in the dielectric medium as well as in the surrounding material.

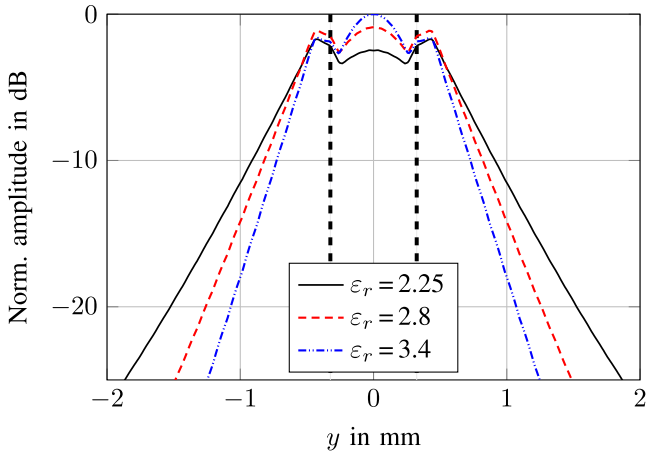

Fig. 5. Simulated E-field distribution of the fundamental HE_{11} mode along the dielectric waveguide center for different dielectric constants. The E-field is polarized in y-direction and normalized to the maximum value.

The field distribution inside and outside the dielectric medium depends on the waveguide dimension and the dielectric constant ε_r. With an increasing cross section the field components in the dielectric increase. Furthermore, a larger dielectric constant decreases the field components in the surrounding medium as shown in Fig. 5. For both cases, the wavenumber β_g increases and the cut-off frequency for higher order modes in the dielectric waveguide becomes lower.

Losses in the waveguide result from dielectric and radiation losses, which depend on the field distribution. For a large wavenumber β_g the field is concentrated in the waveguide and the dielectric losses are high, whereas the radiation losses are high for sparsely concentrated fields in the dielectric waveguide. Parasitic radiation, especially at waveguide bends, is therefore important for a sniffer probe since they can limit the system flexibility.

The dielectric waveguide in the presented system has a rectangular cross section of 648 µm × 1295 µm and is made of high density polyethylene (HDPE, $\varepsilon_{r,\mathrm{HDPE}} = 2.25$, $\tan\delta = 3.1 \cdot 10^{-4}$ at 160 GHz). The dimensions are a compromise between low dielectric losses and high flexibility with low radiation losses, while ensuring a monomodal design. A polarization maintaining rectangular cross section is also beneficial for the mode transformer. If the polarization changes and higher order modes appear, the mode transformer would have a higher insertion loss or would reflect the signal, which would impede the functionality of the sensor. Furthermore, the rectangular cross section is easier to fabricate than other cross sections. In this case a 3 mm thick HDPE plate was thinned to the waveguide width before the tapers were milled.

The losses of the dielectric waveguide were measured in a back-to-back measurement with different waveguide lengths. Fig. 6 shows that the losses increase with frequency, because an increasing part of field is concentrated in the dielectric. For frequencies above 200 GHz a second mode propagates on the waveguide and the linear increasing attenuation is rippled. Compared to theoretically calculated losses [25] in an aluminum rectangular waveguide, the measured losses are

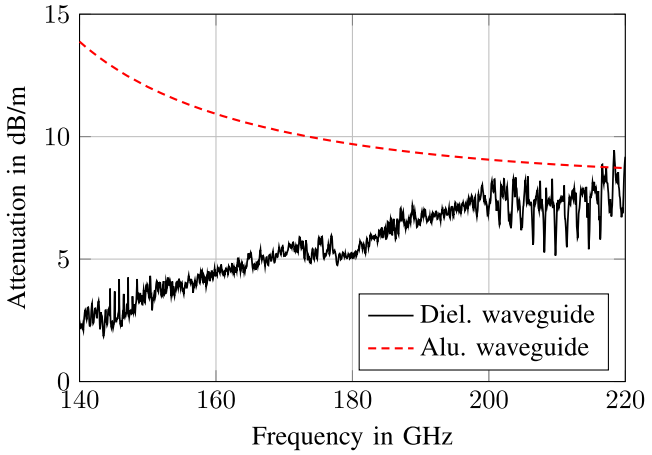

Fig. 6. Measured attenuation for a straight dielectric waveguide made of HDPE and calculated attenuation for an aluminum rectangular waveguide.

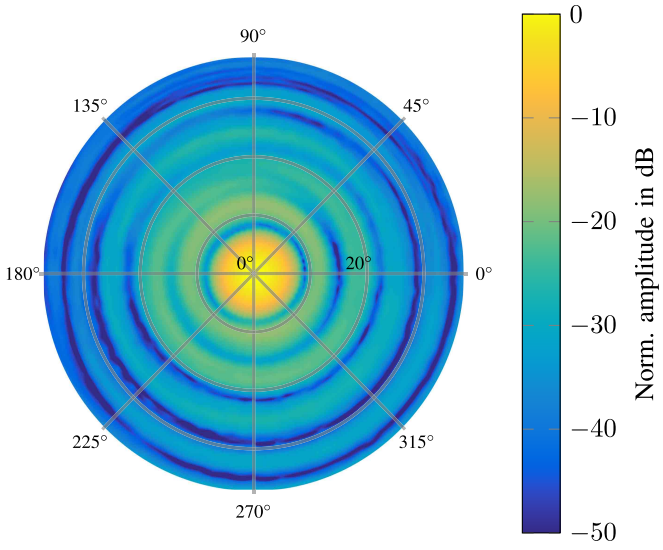

Fig. 7. Measured 3-D radiation pattern at 160 GHz for $R = 7.5$ mm with the H-plane orientation horizontally and the E-plane vertically.

extremely low. Measurements at these frequencies show that the losses in metallic waveguides are considerably larger due to surface roughness, and dielectric waveguides proved to be the lowest loss waveguides for this frequency band.

6) Lens Antenna [21]: For radar applications a high gain antenna is usually needed to achieve a high SNR. Therefore, a dielectric, ellipsoidal lens antenna is plugged on the dielectric waveguide. The lens is fed in its focal point and a widening at the end of the waveguide end improves the matching. For a radius of 7.5 mm the HDPE lens has a gain of 28 dBi. The maximum sidelobe level is below -18.3 dB and the 3 dB angular width is 6.8° in the E-plane and in the H-plane. The measured 3-D radiation pattern at 160 GHz for the elevation angle $-37° < \theta < 37°$ is shown in Fig. 7.

The compact lens directly plugged on the flexible waveguide offers new application areas for radar sensing.

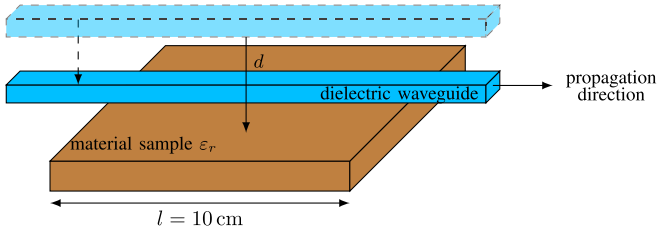

Fig. 8. Measurement setup for the influence of different materials near the dielectric waveguide. The different distances are indicated by the dashed lines.

III. Susceptibility

As the dielectric waveguide influences the system performance decisively, the electrical and mechanical properties are investigated in detail in the following sections.

A. Influence of Surroundings

For the dielectric waveguide with $\varepsilon_{r,\mathrm{HDPE}}$ a surrounding material with a dielectric constant $\varepsilon_r < \varepsilon_{r,\mathrm{HDPE}}$ is assumed. This assumption is fulfilled with air ($\varepsilon_r = 1$) around the waveguide. But in different application scenarios like a radar endoscope, materials with a larger dielectric constant are near the waveguide or even contact the waveguide. Due to the field components outside the waveguide, the field distribution is changed and the transmission characteristics are different. Therefore, this situation is examined with simulations and measurements.

In the measurement setup as shown in Fig. 8, different material samples with a length of $l = 10$ cm were put next to the dielectric waveguide in the H-plane. The transmission and reflection coefficient were measured for different distances d up to 1 mm. The width of the material sample was considerable larger than the waveguide width. The investigated materials can be divided into three groups: metals, dielectric materials with low losses, and absorbers.

A metal sheet near the waveguide has a very low influence on the transmission coefficient. Even for a gap of 1 mm between sheet and waveguide the transmission is hardly influenced. If the metal is in contact with the dielectric waveguide, the transmission decreases by 1 dB to 2 dB. The reason for this characteristic is that most of the field is within the dielectric and only a small part of the energy is reflected and radiated at the metal edges. The metal surface itself limits the field extension in the air and the field distribution is slightly changed.

Dielectric materials have a considerable larger impact on the transmission coefficient. At first materials with low attenuation for frequencies around 160 GHz are considered. The measured attenuation due to the surrounding of the waveguide for three materials with different dielectric constants (HDPE, PREPERM© PP600 ($\varepsilon_r = 6$), PREPERM© L1000HF($\varepsilon_r = 10$) [26]) at 1 mm distance are shown in Fig. 9.

Peaks above 20 dB at different frequencies are visible for all the materials. Between the peaks the attenuation for HDPE and L1000HF is between 0 dB and 1 dB. For PP600 the attenuation is around 5 dB because of a higher dissipation

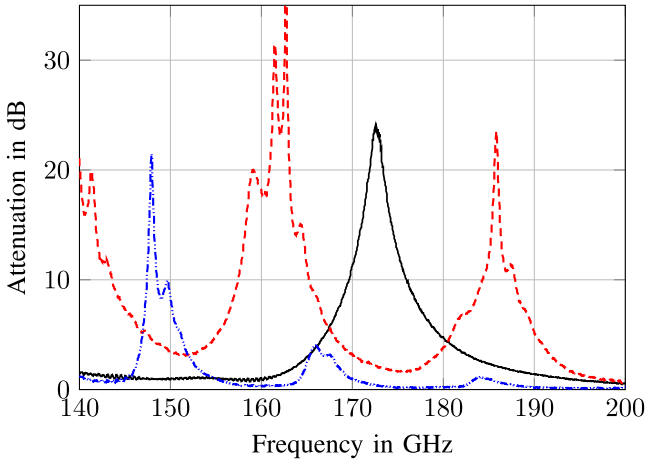

Fig. 9. Measured attenuation for a dielectric waveguide approached 1 mm to HDPE ($\varepsilon_r = 2.25$ (——)), PREPERM© PP600 ($\varepsilon_r = 6$ (- - - -)), and PREPERM© L1000HF ($\varepsilon_r = 10$ (-·-·-·-)) due to coupling and radiation.

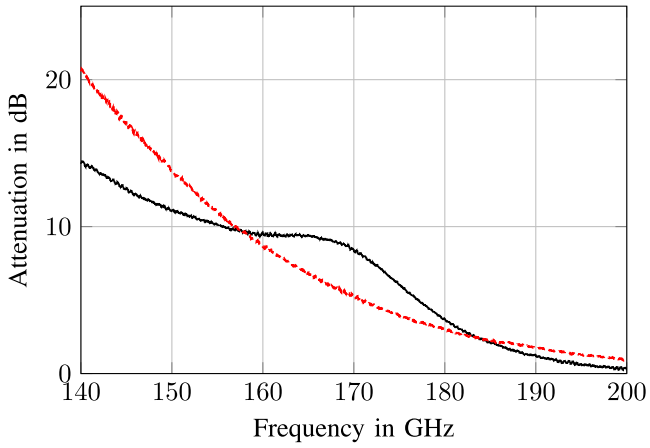

Fig. 10. Measured attenuation for a dielectric waveguide approached 1 mm to materials with cork (——) and absorber (- - - -) due to coupling and radiation.

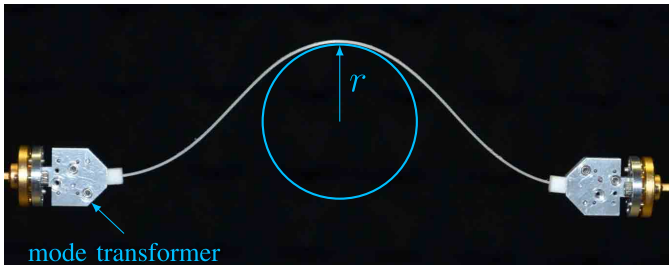

Fig. 11. Measurement setup for the investigation of a bended dielectric waveguide.

factor. The measured curves result from the coupling between the waveguide and the material sample. Along the 10 cm material sample length the wave couples several times between the dielectric waveguide and the material sample, thus there are several attenuation peaks visible. At the peak position all the field energy is in the material sample and almost no energy is in the waveguide. The coupling factor depends on the dielectric constants and their difference, the distance between the material samples and the waveguide, and the frequency [27]. At high frequencies, when most of the energy is concentrated in the waveguide, the attenuation due to the coupling is very small. For distances larger than 2 mm no attenuation is measured since the E-field is 30 dB lower than the maximum value (Fig. 5). For the radar sniffer probe the attenuation implies an attenuated transmit and receive signal. Therefore, the SNR of the radar response deteriorates which impairs the target detection.

The third group of investigated material samples are dielectric materials with a high dissipation factor for mm-waves. These materials are of interest, since the sniffer probe is manually moved during measurements. The electrical properties of a hand ($\varepsilon_r = 58$, $\tan\delta = 0.27$) are approximated with moistened cork and absorber. The measured attenuation for these material samples in 1 mm distance is shown in Fig. 10.

For these materials the wave also couples from the waveguide to the material sample, but due to high dielectric losses, the wave is strongly attenuated in the material sample and only a small part of the energy couples back. Consequently, no peaks are visible since they are less dominant than the attenuation in the material sample. For moistened cork a plateau at 165 GHz gives a hint of a peak at this frequency which is overlapped by the higher attenuation at lower frequencies. Again, the attenuation decreases with increasing frequency as the field components are concentrated in the waveguide for higher frequencies. For larger distances between the material sample and the waveguide the influence is negligible, since the field energy decreases exponentially outside the dielectric material.

B. Influence of Bends

The flexibility of a sniffer probe determines its performance and possible application areas. With the fabricated waveguide bend radii smaller than 1 cm are possible to realize without any permanent mechanical deformation like kinks. But also the electrical properties have to be investigated because of radiation losses in bends [28].

For the measurements of radiation losses in 90° bends, a Rohacell form ($\varepsilon_r = 1.05$) with different radii was used to adjust the minimum radius r of a 20 cm long waveguide as shown in Fig. 11. A permanent fixation with Rohacell resulted in additional dielectric losses and falsified the measurement results.

The radiation losses for the adjusted radii are depicted in Fig. 12. The curves result from the ratio of $|S_{21}|$ measurements with and without bends. With an increasing bend radius, the radiated energy decreases and falls below 1 dB at 140 GHz for the largest radius. Furthermore, the radiation losses depend on frequency. As the field is more concentrated in the dielectric at higher frequencies, the losses due to radiation decrease. In the used frequency range from 146 GHz to 162 GHz the losses for a 1.5 cm bend radius are between 2.1 dB and 0.3 dB. For radii larger than 3 cm the radiated losses are below 0.6 dB and can be neglected for a radar measurement. If the SNR is sufficient for the target detection, even smaller radii can be used. This can be a key benefit to detect targets in areas which are difficult to access.

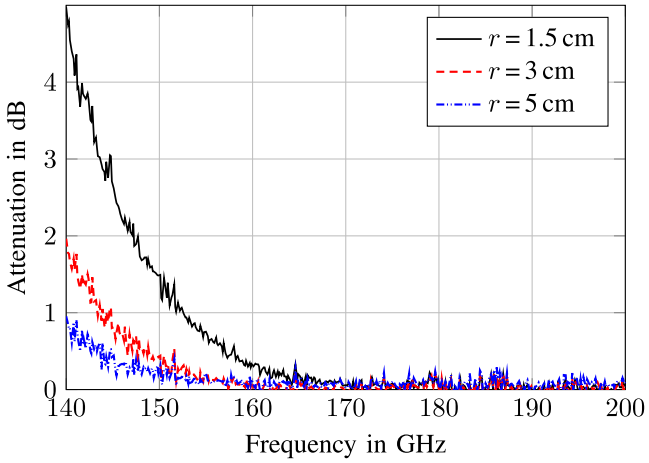

Fig. 12. Measured attenuation in 90° bends from radiation losses for different radii.

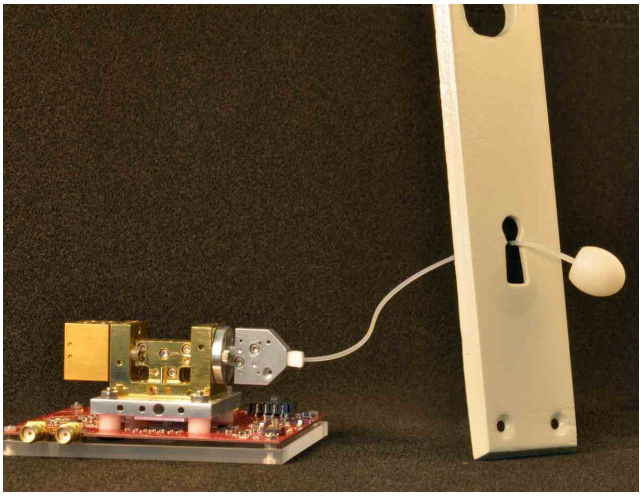

Fig. 13. The sniffer probe is used as endoscope to observe the scenario behind a door. The dielectric waveguide is positioned in the keyhole.

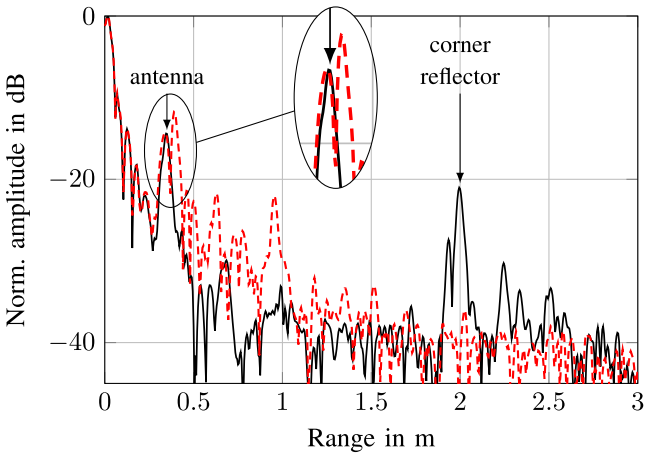

Fig. 14. Range measurement with a sniffer probe and a corner reflector in 1.65 m (——) and 3 cm (- - - -) distance.

Besides the losses in dielectric waveguide bends, the flexibility has also an impact on the phase response which is considerably stronger. However, the phase variation is negligible for range measurements with the sniffer probe since the antenna reflection is used as calibration target to determine the actual distance of real targets to the antenna. The phase and transit time variations on the dielectric waveguide are equal for the calibration and real target. For velocity measurements the phase variations are irrelevant.

C. System SNR

Due to the system extension to a monostatic radar and different transitions, the SNR decreases compared to the bistatic configuration in [18]. The first transition from the MMIC to the metallic waveguide has a loss of 6 dB. In the waveguide coupler the power is splitted in half before the mode transformer attenuates the wave by 0.4 dB. The dielectric waveguide exhibits a loss of 4.5 dB/m. For a corner reflector in 1 m distance with a radar cross section of −3.3 dBsm this would result in a SNR of around 25 dB.

IV. Applications

The presented radar sniffer probe offers many new application areas. The flexible antenna and the spatial separation of radar system and antenna with a low loss connection are the main advantages. In the following sections two new applications for radar measurements with a sniffer probe are exemplified.

A. Radar Sniffer Probe as Endoscope

Endoscope cameras are used to look for pipe blockage or in security applications to observe the scenario behind a wall or door. But a camera does not give any information about the range or velocity of the observed object. A radar system combined with a camera provides a picture of the scenario and the corresponding information.

Up to now, radar systems are usually mounted on PCBs and are thus too large to being pushed through pipes or small apertures. The flexible and small dielectric waveguide with a lens antenna enables the usage of a radar system with an endoscope camera as described. In Fig. 13 a measurement scenario through a keyhole is shown, in which the dielectric waveguide is positioned in a keyhole and the lens is plugged afterwards. For this measurement a corner reflector that was positioned at a distance of 1.65 m from the antenna was used as a target. The measured radar response for the scenario is depicted in Fig. 14. The corner reflector is measured at 2 m since the length of the dielectric waveguide is not subtracted. The peak at 35 cm is the reflection at the antenna and far away from the DC peak resulting from crosstalk. Therefore, targets with short distances to the antenna can also be measured as shown in the second measurement (- - - -) with a corner reflector at a distance of 3 cm. The repetitive targets in the second measurement results from multiple reflections. Due to the large distance between sensor and antenna and the high bandwidth of 16 GHz, the antenna appears in the 35$^{\text{th}}$ range cell. Thus, DC offset and leakage are no limiting factors for the close range measurement performance.

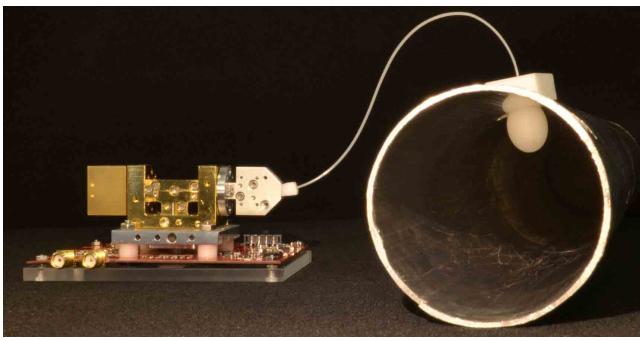

Fig. 15. Volume flow measurement with sniffer probe in a pipe. Only a small hole is needed for the antenna.

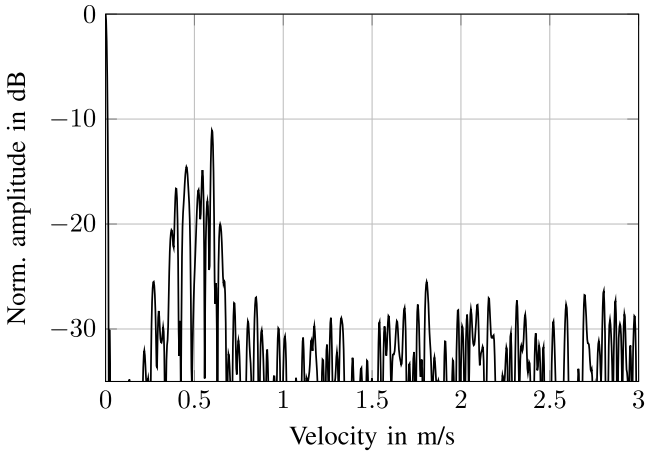

Fig. 16. Velocity measurement with a sniffer probe in a metal pipe to determine the volume flow of water. Multiple peaks are visible due to the turbulent stream current.

B. Radar Sniffer Probe for Volume Flow Measurement in Pipes

Radar systems are used to measure the volume flow for fluids in rivers or solids in large pipes [29]. For these measurements the pipes have an opening to position the antenna with the radar system over the pipe. For a large antenna aperture size a large opening in the pipe is needed which is undesired in applications with steaming or corrosive fluids.

With a radar sniffer probe only a small hole in the pipe is needed and the lens antenna can be positioned with high accuracy. The radar system PCB is not affected by the fluids and can be positioned in a dry and normally tempered surroundings. The known measurement scenarios like the volume flow in large pipes with fluids are extended with the sniffer probe. New applications are the volume flow measurements in small, partly filled pipes for fluids or even solids like screws in industrial applications and grain in agricultural applications.

In a measurement setup with the sniffer probe in a metal pipe as shown in Fig. 15 the velocity of water through a pipe was measured. The sniffer probe radar is used as a CW radar to determine the velocity. In Fig. 16 the measured velocity of the partly filled pipe is shown. The multiple peaks around 0.5 m/s result from the turbulent stream current in the pipe.

V. Conclusion

In this paper a novel 160 GHz radar system is presented, which enables radar measurements around obstacles or at inaccessible and harsh surroundings. The flexible and compact sniffer probe offers completely new application areas for radar systems.

For the transition from the bistatic 160 GHz MMIC with 16 GHz bandwidth to the monostatic sniffer probe a metallic waveguide duplexer is used, which is connected to the chip using a MMIC-to-metallic waveguide transition. The main part of the system, the flexible dielectric waveguide made of HDPE, is fed by a widened metallic waveguide. The dielectric waveguide supports bending radii of up to 1.5 cm with negligible losses and can be approached to other materials without losses up to 2 mm. With an attenuation of 4.5 dB/m at 160 GHz the extremely low loss dielectric waveguide can connect the high gain dielectric lens antenna with the MMIC over a large distance. The lens has a gain of 28 dBi and a compact radius of 7.5 mm. Thus the dynamic range of the system is completely sufficient for typical short range sniffer probe applications.

The two presented sniffer probe applications show only a small selection of the versatile possibilities for which the radar sniffer probe can be used.

References

[1] D. Brumbi, "Low power FMCW radar system for level gaging," in *IEEE MTT-S Int. Microw. Symp. Dig.*, vol. 3, Jun. 2000, pp. 1559–1562.

[2] J. Hatch, A. Topak, R. Schnabel, T. Zwick, R. Weigel, and C. Waldschmidt, "Millimeter-wave technology for automotive radar sensors in the 77 GHz frequency band," *IEEE Trans. Microw. Theory Techn.*, vol. 60, no. 3, pp. 845–860, Mar. 2012.

[3] F. Bauer, X. Wang, W. Menzel, and A. Stelzer, "A 79-GHz radar sensor in LTCC technology using grid array antennas," *IEEE Trans. Microw. Theory Techn.*, vol. 61, no. 6, pp. 2514–2521, Jun. 2013.

[4] C. Beck *et al.*, "Industrial mmWave radar sensor in embedded wafer-level BGA packaging technology," *IEEE Sensors J.*, vol. 16, no. 17, pp. 6566–6578, Sep. 2016.

[5] M. Jahn, R. Feger, C. Wagner, Z. Tong, and A. Stelzer, "A four-channel 94-GHz SiGe-based digital beamforming FMCW radar," *IEEE Trans. Microw. Theory Techn.*, vol. 60, no. 3, pp. 861–869, Mar. 2012.

[6] T. Spreng, S. Yuan, V. Valenta, H. Schumacher, U. Siart, and V. Ziegler, "Wideband 120 GHz to 140 GHz MIMO radar: System design and imaging results," in *Proc. Eur. Microw. Conf. (EuMC)*, Sep. 2015, pp. 430–433.

[7] J. Grzyb, K. Statnikov, N. Sarmah, B. Heinemann, and U. R. Pfeiffer, "A 210–270-GHz circularly polarized FMCW radar with a single-lens-coupled SiGe HBT chip," *IEEE Trans. THz Sci. Technol.*, vol. 6, no. 6, pp. 771–783, Nov. 2016.

[8] M. Hitzler, S. Saulig, L. Boehm, W. Mayer, W. Winkler, and C. Waldschmidt, "Compact bistatic 160 GHz transceiver MMIC with phase noise optimized synthesizer for FMCW radar," in *IEEE MTT-S Int. Microw. Symp. Dig.*, May 2016, pp. 1–4.

[9] T. Jaeschke, C. Bredendiek, and N. Pohl, "A 240 GHz ultra-wideband FMCW radar system with on-chip antennas for high resolution radar imaging," in *IEEE MTT-S Int. Microw. Symp. Dig.*, Jun. 2013, pp. 1–4.

[10] M. Furqan, F. Ahmed, R. Feger, K. Aufinger, and A. Stelzer, "A 120-GHz wideband FMCW radar demonstrator based on a fully-integrated SiGe transceiver with antenna-in-package," in *Proc. IEEE MTT-S Int. Conf. Microw. Intell. Mobility (ICMIM)*, May 2016, pp. 1–4.

[11] B. Göttel, M. Pauli, H. Gulan, M. Girma, J. Hasch, and T. Zwick, "Miniaturized 122 GHz short range radar sensor with antenna-in-package (AiP) and dielectric lens," in *Proc. 8th Eur. Conf. Antennas Propag. (EuCAP)*, Apr. 2014, pp. 709–713.

[12] S. Thomas, C. Bredendiek, T. Jaeschke, F. Vogelsang, and N. Pohl, "A compact, energy-efficient 240 GHz FMCW radar sensor with high modulation bandwidth," in *Proc. German Microw. Conf. (GeMiC)*, Mar. 2016, pp. 397–400.

[13] Y. C. Ou and G. M. Rebeiz, "On-chip slot-ring and high-gain horn antennas for millimeter-wave wafer-scale silicon systems," *IEEE Trans. Microw. Theory Techn.*, vol. 59, no. 8, pp. 1963–1972, Aug. 2011.
[14] H. Kudo *et al.*, "Fiber optic bio-sniffer (biochemical gas sensor) using UV-LED light for monitoring ethanol vapor with high sensitivity & selectivitiy," in *Proc. IEEE SENSORS*, Oct. 2009, pp. 1955–1958.
[15] J. Weinzierl, C. Fluhrer, and H. Brand, "Dielectric waveguides at submillimeter wavelengths," in *Proc. IEEE 6th Int. Conf. Terahertz Electron.*, Sep. 1998, pp. 166–169.
[16] N. Van Thienen, W. Volkaerts, and P. Reynaert, "A multi-gigabit CPFSK polymer microwave fiber communication link in 40 nm CMOS," *IEEE J. Solid-State Circuits*, vol. 51, no. 8, pp. 1952–1958, Aug. 2016.
[17] J. W. Holloway, L. Boglione, T. M. Hancock, and R. Han, "A fully integrated broadband sub-mmWave chip-to-chip interconnect," *IEEE Trans. Microw. Theory Techn.*, vol. 65, no. 7, pp. 2373–2386, Jul. 2017.
[18] M. Hitzler *et al.*, "Ultracompact 160-GHz FMCW radar MMIC with fully integrated offset synthesizer," *IEEE Trans. Microw. Theory Techn.*, vol. 65, no. 5, pp. 1682–1691, May 2017.
[19] M. Hitzler, S. Saulig, L. Boehm, W. Mayer, and C. Waldschmidt, "MMIC-to-waveguide transition at 160 GHz with galvanic isolation," in *IEEE MTT-S Int. Microw. Symp. Dig.*, May 2016, pp. 1–4.
[20] M. Hitzler, J. Iberle, W. Mayer, H. Barth, and C. Waldschmidt, "Wide-band low-cost hybrid coupler for mm-wave frequencies," in *IEEE MTT-S Int. Microw. Symp. Dig.*, May 2017.
[21] M. Geiger, M. Hitzler, J. Iberle, and C. Waldschmidt, "A dielectric lens antenna fed by a flexible dielectric waveguide at 160 GHz," in *Proc. 11th Eur. Conf. Antennas Propag. (EuCAP)*, Mar. 2017, pp. 3380–3383.
[22] A. Standaert and P. Reynaert, "Analysis of hollow circular polymer waveguides at millimeter wavelengths," *IEEE Trans. Microw. Theory Techn.*, vol. 64, no. 10, pp. 3068–3077, Oct. 2016.
[23] K. C. Kao and G. A. Hockham, "Dielectric-fibre surface waveguides for optical frequencies," *Proc. Inst. Elect. Eng.*, vol. 113, no. 7, pp. 1151–1158, Jul. 1966.
[24] E. A. J. Marcatili, "Dielectric rectangular waveguide and directional coupler for integrated optics," *Bell Syst. Tech. J.*, vol. 48, no. 7, pp. 2071–2102, Sep. 1969.
[25] R. E. Collin, *Foundations for Microwave Engineering* (IEEE Press Series on Electromagnetic Wave Theory). Hoboken, NJ, USA: Wiley, 2001.
[26] *PREPERM L1000HF*, Premixgroup, Rajamäki, Finland, Dec. 2013.
[27] K. J. Ebeling, *Integrierte Optoelektronik: Wellenleiteroptik, Photonik, Halbleiter*. Berlin, Germany: Springer, 1989.
[28] E. A. J. Marcatili, "Bends in optical dielectric guides," *Bell Syst. Tech. J.*, vol. 48, no. 7, pp. 2103–2132, Sep. 1969.
[29] C. Baer, T. Jaeschke, P. Mertmann, N. Pohl, and T. Musch, "A mmWave measuring procedure for mass flow monitoring of pneumatic conveyed bulk materials," *IEEE Sensors J.*, vol. 14, no. 9, pp. 3201–3209, Sep. 2014.

Martin Geiger (S'16) received the M.Sc. degree from Ulm University, Ulm, Germany, in 2015, where he is currently pursuing the Ph.D. degree.

In 2016, he joined the Institute of Microwave Engineering, Ulm University. His current research interests include novel radar sensor concepts with flexible antennas, dielectric waveguides, and MMIC interconnects, all at millimeter-wave frequencies.

Martin Hitzler (S'13) received the Dipl.Ing. degree in electrical engineering from Ulm University, Ulm, Germany, in 2012, where he is currently pursuing the Ph.D. degree.

In 2013, he joined the Institute of Microwave Engineering, Ulm University. His current research interests include FMCW radar sensors, integrated antennas, MMIC packaging, and interconnects, all at millimeter-wave frequencies.

Mr. Hitzler was a recipient of the ARGUS Science Award in 2013.

Stefan Saulig (S'16) received the B.Eng. degree in information and communications technology and the M.Sc. degree in computer controlled systems from the Aalen University of Applied Sciences, Aalen, Germany, in 2009 and 2011, respectively. He is currently pursuing the Ph.D. degree with the Institute of Microwave Engineering, University of Ulm, Ulm, Germany.

He was in an apprenticeship to a Skilled Manual Worker with Radio Technology, German Armed Forces, Germany, from 1997 to 2001. He operated as a Soldier with a focus on radar technology with a German NATO Base from 2001 to 2009. From 2011 to 2013, he was involved in systems and safety engineering with Robert Bosch Automotive Steering GmbH, Schwäbisch Gmünd, Germany. In 2013, he joined the Institute of Microwave Engineering, University of Ulm. Since 2016, he has been with Robert Bosch Automotive Steering GmbH, as a Project Leader, where he is involved in the product engineering for system development and requirement management. His current research interests include multichannel imaging radar systems at 160 GHz.

Johannes Iberle received the B.Eng. degree in communications engineering from the Ulm University of Applied Sciences, Ulm, Germany, in 2013, and the M.Sc. degree in electrical engineering from Ulm University, Ulm, in 2016.

In 2016, he joined the Laboratory of Microtechnology, University of Applied Sciences, Ulm, as a Research Assistant. His current research interests include micro doppler effects in radar and radar target simulators for automotive radar sensors.

Philipp Hügler (S'15) received the M.Sc. degree from Ulm University, Ulm, Germany, in 2014, where he is currently pursuing the Ph.D. degree with the Institute of Microwave Engineering. His research focuses on close-up range FMCW radar sensors and imaging radar front-ends at millimeter-wave frequencies.

Christian Waldschmidt (S'01–M'05–SM'13) received the Dipl.Ing. (M.S.E.E.) and Dr.-Ing. (Ph.D.E.E.) degrees from the University of Karlsruhe (TH), Karlsruhe, Germany, in 2001 and 2004, respectively. From 2001 to 2004, he was a Research Assistant with the Institut für Höchstfrequenztechnik and Elektronik, University of Karlsruhe (TH). Since 2004, he has been with Robert Bosch GmbH, in the business units Corporate Research and Chassis Systems. He was heading different research and development teams in microwave engineering, rf-sensing, and automotive radar.

In 2013, he returned to academia. He was appointed as the Director of the Institute of Microwave Engineering, University Ulm, Germany, as a Full Professor. He has authored or co-authored over 100 scientific publications and over 20 patents. The research topics focus on radar and rf-sensing, mm-wave and submillimeter-wave engineering, antennas and antenna arrays, and rf and array signal processing. He is the Vice Chair of the IEEE MTT-27 Technical Committee (wireless enabled automotive and vehicular applications), the Executive Committee Board Member of the German MTT/AP Joint Chapter, and a member of the ITG Committee Microwave Engineering. In 2015, he served as the TPC Chair of the IEEE Microwave Theory and Techniques Society International Conference on Microwaves for Intelligent Mobility. He is a reviewer for multiple IEEE TRANSACTIONS and letters.